POAC'25
St. John's, Newfoundland and Labrador, Canada

Proceedings of the 28th International Conference on Port and Ocean Engineering under Arctic Conditions
Jul 13-17, 2025
St. John's, Newfoundland and Labrador
Canada

Experimental study on the ice resistance in ship, ice and regular wave interaction

Junji Sawamura [1], Akihisa Konno [2], Taiki Tokudome [2]
[1] Department of Naval Architecture and Ocean Engineering, Osaka University (Osaka, JAPAN)
[2] Department of Mechanical Engineering, Kogakuin University (Tokyo, JAPAN)

ABSTRACT

This paper presents a model test using synthetic ice to measure the ice force acting on the hull as ship advances through an ice channel with small ice floes and regular wave. Disk-shaped synthetic ice made of polypropylene (PP) was used. The model ship was towed by the towing carriage at a constant speed through the ice channel with ice-wave interactions. The ice and wave force acting on the model ship, as well as the motion of ice floes near the bow, were measured. The forces measured during ship-ice-wave interaction were compared with those obtained during ship-ice interaction in order to experimentally investigate the effect of the regular wave on the ice force. Furthermore, the relationship between the motion of ice floes near the bow and the ice force was analyzed. The differences in ice resistance between conditions with and without regular waves were small, as the average collision speed of ice floes at the bow was similar in both conditions. However, the peak forces experienced during regular wave conditions were greater than those without regular waves (calm water), due to increased collision speeds caused by wave-induced ice floe motions. These results indicate that wave effects on ship-ice interactions are significant and should be carefully considered in the design of ice-going ships.

KEY WORDS: Ship-ice-wave interaction; Ice force; Ice floe motion; Model test.

INTRODUCTION

When designing ice-going ships, it is essential to understand ship-ice interactions when a ship collides with sea ice. A ship crossing the Northern Sea Route (NSR) inevitably sails through marginal ice zones (MIZs), where many ice floes of varying sizes are dispersed. Due to the recent worsening of wave climate caused by the shrinking of ice extent in the Arctic, the motion of ice floes may increase as a result of higher waves (Khon et al., 2014). For safe operation in the MIZ, it is necessary to understand the motion of ice floes in waves and to accurately estimate the ice forces on ships under waves, i.e., ship-ice-wave interactions.

Wave-ice interaction has been studied for many years, but there are few studies related to ship-ice-wave interactions. Zou et al. (2022), Tang et al. (2022), and Huang et al. (2020, 2021) used a CFD-DEM coupling method to calculate the ice forces, including the effect of wave generation, when a ship moves forward through pack ice floes. Model testing in an ice tank is necessary for the design of ice-going vessels. However, model tests in an ice tank require high experimental skill and cost, especially for ice-wave interactions. Therefore, model tests using synthetic ice have been proposed as an alternative method, reducing both experimental skill requirements and costs by using a general towing tank. Luo et al. (2018) conducted model tests to investigate the effect of waves on ice resistance for ships navigating through small pack ice floes. In these tests, wax synthetic ice was used, and the tests were conducted in a towing tank instead of an ice tank. Sawamura et al. (2018) also conducted model tests to estimate ice resistance (average ice force) in ship-wave-ice interactions using polypropylene (PP) synthetic ice. The results showed that the ice resistance measured with regular waves was slightly smaller than that without regular waves. This result may be due to the different ice motion near the ship bow during ship-ice-wave interactions, compared to ship-ice interactions. However, the motion of ice floes near the bow was not been measured in the model test of Sawamura et al. (2018), therefore the exact reasons have not been identified.

This paper presents model tests using PP synthetic ice to measure the ice forces when a ship advances through an ice channel with small ice floes and regular waves. The forces acting on the model ship and the motion of ice floes (vertical displacement and horizontal velocity) near the ship's bow during ship-ice-wave interactions were measured. The measured forces and ice floe motions in ship-ice-wave interactions were compared with those in ship-ice interactions. Furthermore, the peak ice forces and ice motions at different wave heights are presented. The effect of regular waves on ice forces was investigated experimentally.

EXPERIMENTAL SETUP

Model tests using synthetic ice were conducted in a towing tank at Osaka University, Japan. The towing tank is 100 m in length, 7.8 m in width, and 4.35 m in depth. The experimental area was between 40 m and 55 m in length and 2 m in width. Floats were used to create an ice-covered channel in the center of the towing tank. Each float was connected by a flexible rope. The motion of the ice floes in the ice channel was gently restricted by the floats. Sawamura et al. (2016) confirmed that the presence of the floats had little effect on the ice resistance in model tests of ship-ice interaction without waves, even when the width of the ice channel was varied. The water surface in front of the model ship, approximately 10 m long and 2 m wide, was covered with 4500 ice floes. A simplified model ship, made from polyvinyl chloride (PVC) plates, was used. The principal dimensions of the model are 1.75 m in length, 0.30 m in width, and 0.078 m in draft. The stem and waterline entrance angles of the bow are 30° and 30°, respectively. The model ship was designed at a scale of approximately 1:100. However, the model was not designed using actual ship dimensions. The model ship was a flexural model capable of measuring longitudinal deformation during ship-ice-wave interactions. However, the measured flexural deformation is not presented in this paper. Disk-shaped polypropylene (PP) ice was used as the ice floes. The thickness and diameter of the PP synthetic ice were 0.01 m and 0.05 m, respectively. The ice concentration was approximately 78% when the ice floes were uniformly distributed without any gaps. However, the ice concentration in the tests varied spatially due to the drift of the ice floes caused by the waves and ship movement, as well as the presence of gaps between the ice

floes during the measurements. The ice concentration near the ship bow in the experiment could be calculated using image analysis based on image data of the ice floes' movement near the bow, but this was not provided in this paper. The density of PP is 910 kg/m³, similar to that of sea ice. The friction coefficient between the ship model (PVC) and the ice (PP) was not measured in the experiment. The static friction coefficients of 0.4 (for PVC) and 0.3 (for PP) in dry conditions are listed in the respective product catalogs.

The model ship was rigidly fixed to the towing carriage via a towing rod at the midship and advanced in a straight line at constant speeds of 0.2, 0.3, and 0.4 m/s. Ship motions were not considered. A load cell (LMC-3502A-10N, Nissho Electric Works Co., Ltd.) was attached between the model ship and the towing carriage. Surge, heave, and pitch moment were measured with a sampling frequency of 1 kHz. A video camera mounted above the ship's bow recorded the horizontal movement of the ice floes near the bow within an area measuring 1.2 m in length and 0.7 m in width. The horizontal velocity of the ice floes was obtained by image processing using the commercial software TEMA LITE T2021a. The vertical displacement of the ice floes (ice floe height) near the bow was measured using a CMOS laser sensor (IL600, Keyence Corp.). Three wave heights of 0.02, 0.03, and 0.04 m, and one wavelength of 1.33 m, were selected for the regular waves. The wave height outside the ice channel in front of the ship’s bow was measured by a capacitance-type wave height meter (CHT7-10E, Kenek Co., Ltd.). Table 1 shows the experimental wave and ice floe conditions. Fig. 1 shows the experimental setup. The test was repeated three times under each test condition to verify the accuracy of the measurements. The model tests were conducted both in ice-covered water and in open water. The ice force related to the ice floes was obtained by subtracting the measured force in open water from that in ice-covered water.

Table 1. Experimental conditions.

Test	Wave length [m]	Wave height [m]	Ice floes [pieces]	Carriage speed [m/s]	Condition
01				0.2	Calm water (Open water)
02				0.3	
03				0.4	
04	1.33	0.02		0.2	Regular wave (Open water)
05	1.33	0.02		0.3	
06	1.33	0.02		0.4	
07	1.33	0.03		0.3	
08	1.33	0.04		0.3	
09			4500	0.2	Ice floes + Calm water
10			4500	0.3	
11			4500	0.4	
12	1.33	0.02	4500	0.2	Ice floes + Regular wave
13	1.33	0.02	4500	0.3	
14	1.33	0.02	4500	0.4	
15	1.33	0.03	4500	0.3	
16	1.33	0.04	4500	0.3	

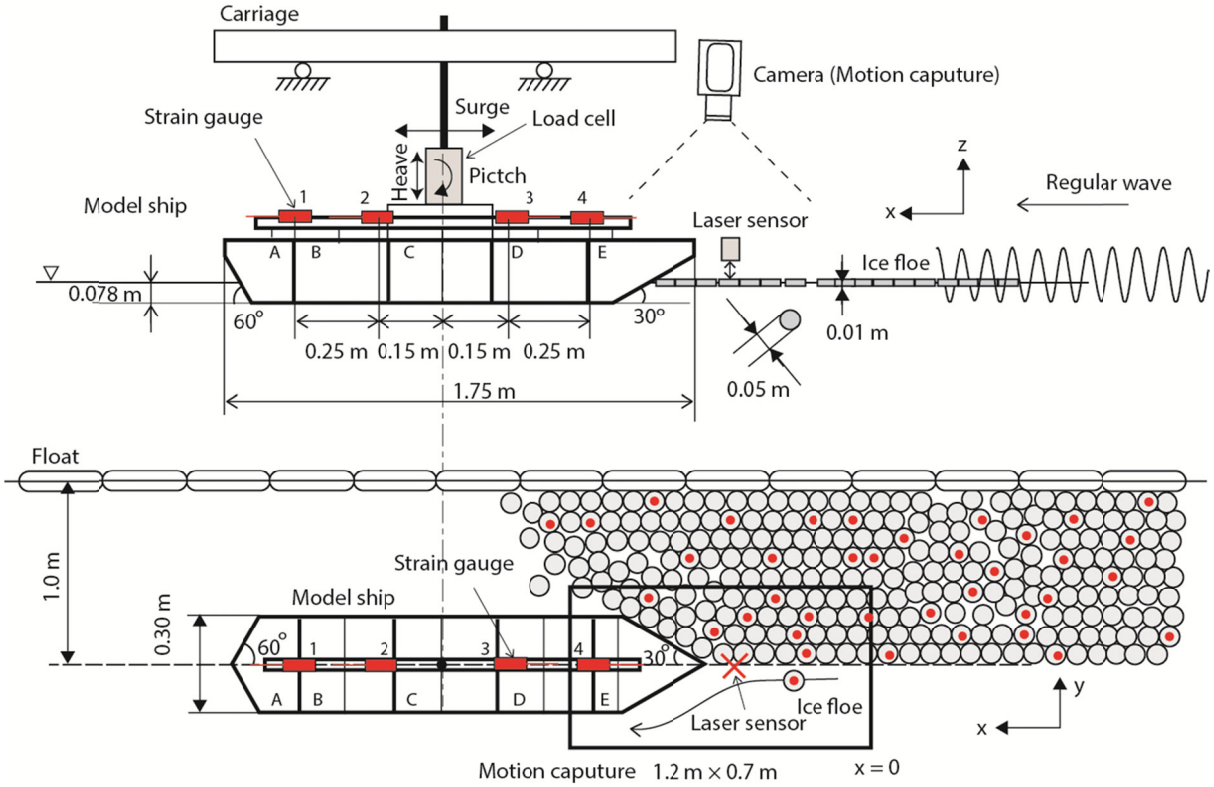

Figure 1. Experimental setup.

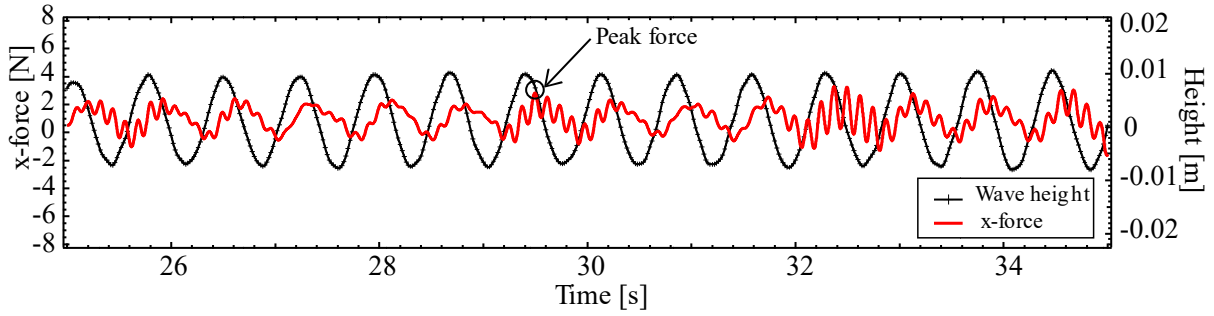

(a) Test 05 (without ice floes)

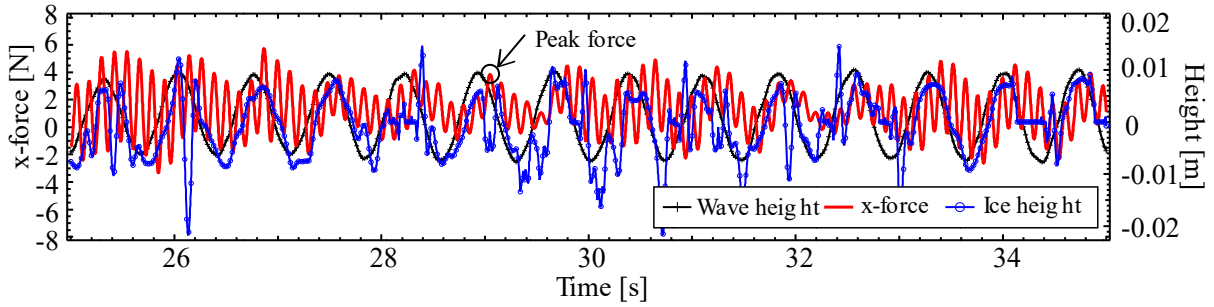

(a) Test 13 (with ice floes)

Figure 2.Time history of the measured surge ice force (x-direction), wave and ice height with (a) and without ice floes (b) (Wave length = 1.33 m, wave height = 0.02 m, and ship speed = 0.3 m/s).

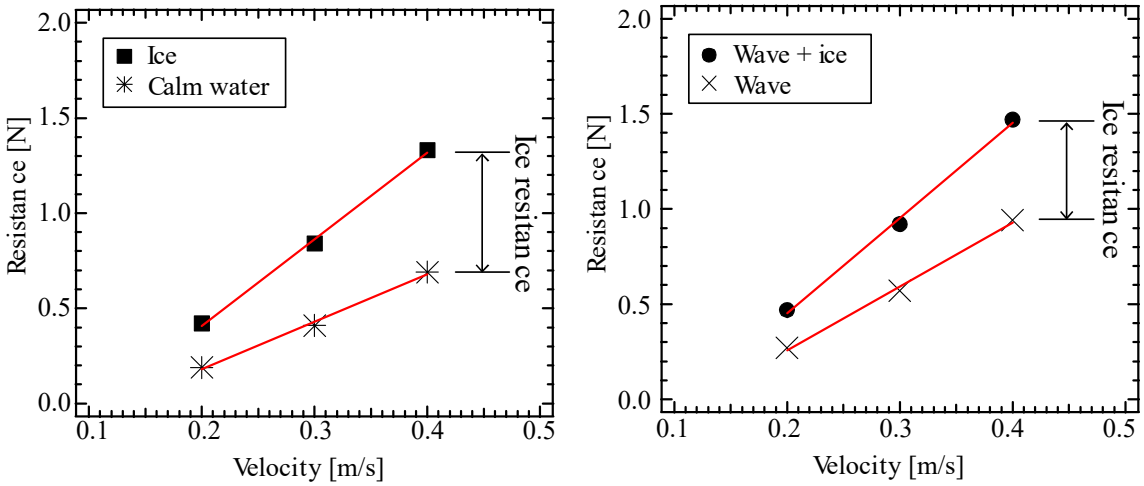

(a) Calm water
(Test01, 02, 03, 09, 10 and 11)

(b) Regular wave
(Test04, 05, 06, 12, 13 and 14)

Figure 3. Relationship between the carriage speed and the average force (resistance) in calm water (Tests 01, 02, 03, 09, 10, and 11) and in regular waves (Tests 04, 05, 06, 12, 13, and 14).

EXPERIMENTAL RESULTS

Measured ice force and ice motion in ship-ice-wave interaction

Fig. 2 presents example time histories of the measured surge force (x-direction), wave height, and ice wave height when the model ship advances in regular waves without ice floes (Test05) and with ice floes (Test13). In this paper, the measured data after applying a 10 Hz low-pass filter are shown. The time histories of the ice force, both with and without ice floes, show that small-period vibrations are included in the long-period vibration induced by the wave. These small vibrations were caused by the natural frequency of the flexural model ship. However, the small vibrations with ice floes (Test13) show larger fluctuations than those without ice floes (Test05), caused by ice floe collisions. These results suggest that the effect of wave and ice interactions is significant on the ice force acting on the model ship. The ice wave height in ship-ice-wave interaction (Test13) becomes slightly smaller than the wave height (the inlet regular wave) due to the attenuation of the wave in the ice channel. Since the laser sensor cannot measure the water surface, the ice height data was frequently lost due to gaps between the ice floes, as shown in Fig. 2b. Improvements in the experimental setup are necessary to measure the accurate ice wave height.

Fig. 3 shows the relationship between the carriage speed and the ice resistance (average ice force) in calm water (without ice: Tests 01, 02, 03, with ice: Tests 09, 10, and 11) and in regular waves (without ice: Tests 04, 05, 06, with ice: Tests 12, 13, and 14). Tables 2 and 3 show the ice resistance in calm water and in regular waves, respectively. In Table 3, the measured wave height (Tests 04, 05, 06) and ice wave height (Tests 12, 13, 14) are also inclused. In this paper, the ice force in the ice channel F_{ice} is calculated by subtracting the measured force in open water $F_{\text{open water}}$ from the force in the ice channel $F_{\text{ice channel}}$. The resistance force (R_{ice}, $R_{\text{open water}}$, $R_{\text{ice channel}}$) was calculated by averaging the measured force during the experiment.

$$F_{\text{ice}}(R_{\text{ice}}) = F_{\text{ice channel}}(R_{\text{ice channel}}) - F_{\text{open water}}\left(R_{\text{open water}}\right), \text{in wave or calm water} \quad (1)$$

Table 2. Ice resistance in calm water.

Velocity	Measured resistance (F_{total})		Ice resistance (F_{ice})	Test No.
[m/s]	[N]		[N]	
	Open water	Ice floes	Open – Ice	
0.2	0.19	0.42	0.23	Test09 – Test01
0.3	0.41	0.84	0.44	Test10 – Test02
0.4	0.69	1.33	0.64	Test11 – Test03

Table 3. Ice resistance in the regular wave (wave height = 0.02 m).

Velocity	Measured resistance (F_{total})		Ice resistance (F_{ice})	Height		Test No.
[m/s]	[N]		[N]	[m]		
	Wave water	Ice + wave	Ice – Wave	Wave	Ice	
0.2	0.27	0.47	0.20	0.017	0.014	Test12 – Test04
0.3	0.57	0.92	0.35	0.016	0.015	Test13 – Test05
0.4	0.94	1.47	0.53	0.014	0.014	Test14 – Test06

In Fig.3, the resistance force in all test cases increases proportionally as the ship speed increases. The resistance force in the ice channel (■, ●) is greater than that in the open water (*, ×) in both calm water (Fig.3a) and regular wave (Fig.3b) due to the ice collisions. The ice resistance obtained from Eq. (1) increases proportionally as the ship speed increases, both in calm water and regular waves. Additionally, the ice resistance (i.e., differences between the resistance with ice floes and that without ice floes) in the calm water becomes larger than that in regular wave. This result is consistent with the findings of Sawmura et al. (2018), and might be caused by the discrepancy between wave height and ice height. To apply Eq. (1) correctly, the heights of the regular wave and the ice wave must be consistent. However, due to attenuation in the ice channel, the ice wave heights in Tests 12, 13, and 14 are slightly lower than those in Tests 04, 05, and 06.

Fig. 4 shows the ice relative velocity in x-direction near the ship bow (1.2 m × 0.7 m) in the calm water (Tests 09, 10, and 11) and regular wave conditions (Tests 12, 13, and 14) at different ship speeds. In Fig.4, the ice velocities of 12 floes (Ice01- 12) are shown, and the trend line for Ice05 is additionally included. The bow is located at x = 0.74 m in the horizontal axis, and the ice floes move toward the ship from x = 0.0 m. In calm water (Figs. 4a, 4b, and 4c), the relative ice velocity at x = 0.0 m is approximately equal to the ship speed and gradually decreases as the ice floes approach the model ship. This is because the advancing ship pushes the ice floes in the negative x-direction. In regular wave conditions (Figs. 4d, 4e, and 4f), the ice velocity fluctuates due to wave motion but also decreases as the ice floes approach the ship. The positive and negative peaks of the ice velocity are larger under regular wave conditions than in calm water. Nevertheless, the overall trend line of the ice velocity in regular waves closely resembles that in calm water. This result suggests that the ice resistance in regular wave conditions is approximately equal to that in calm water, as the average ice collision velocity shows similar trend in both cases. Fig. 5 shows the peak force measured in open water (Tests 04, 05, and 06) and in the ice channel (Tests 12, 13, and 14). The peak ice force in regular wave conditions, calculated using Eq. (1), is significantly higher due to the increased collision velocity compared to that in calm water..

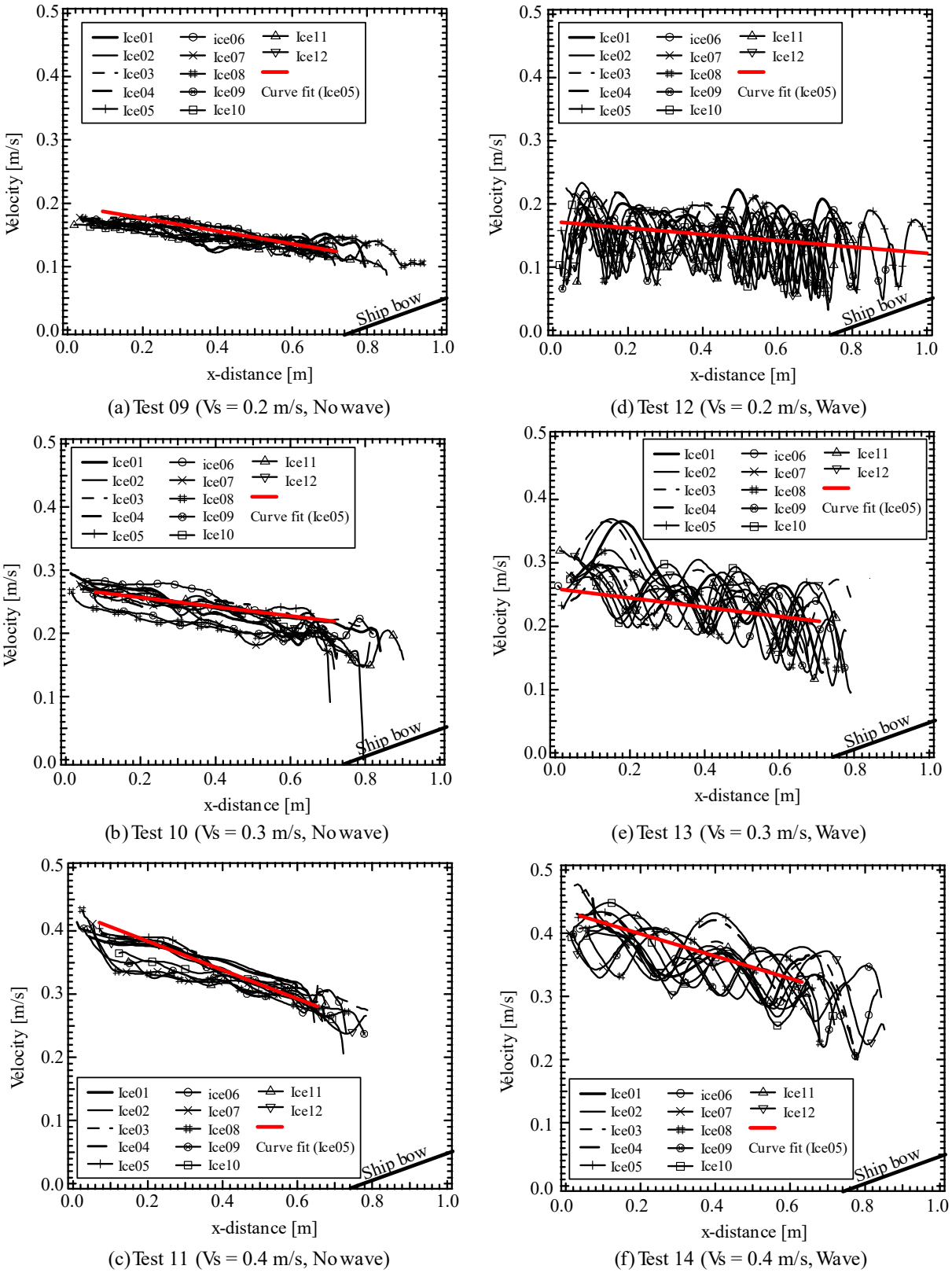

(a) Test 09 (Vs = 0.2 m/s, No wave)

(b) Test 10 (Vs = 0.3 m/s, No wave)

(c) Test 11 (Vs = 0.4 m/s, No wave)

(d) Test 12 (Vs = 0.2 m/s, Wave)

(e) Test 13 (Vs = 0.3 m/s, Wave)

(f) Test 14 (Vs = 0.4 m/s, Wave)

Figure 4. Ice relative velocity (x-direction) near the ship bow in calm water (Test09, 10, and 11) and regular wave (Test12, 13, and 14) in different ship speed.

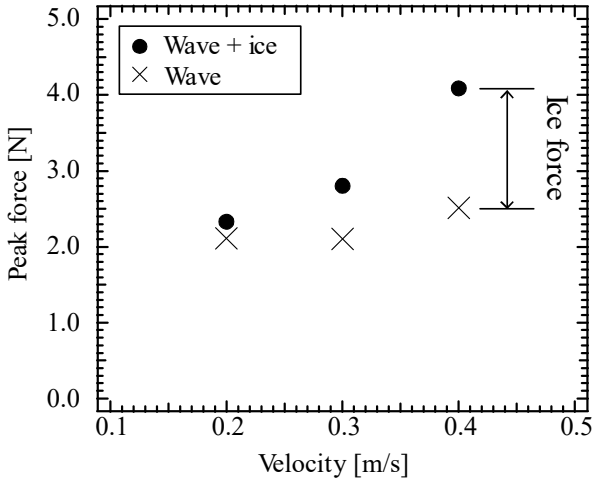

Figure 5. Relationship between ship velocity and the peak force in the regular wave (Test04, 05, and 06) and regular wave + ice floes (Test12, 13, and 14).

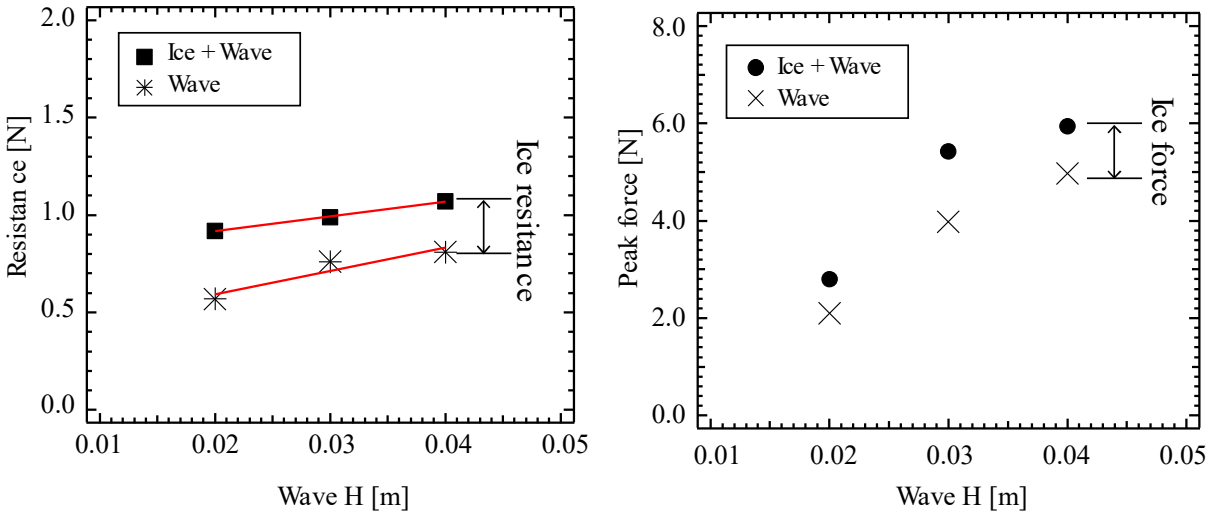

(a) Average force (resistan ce) (b) Peak force

Figure 6. Average force (resistance) and peak force in the regular wave (Test05, 07, and 08) and regular wave + ice floes (Test13, 15, and 16) in different wave height.

Table 4. Ice resistance in the regular wave (ship velocity = 0.3 m/s).

Wave H	Measured resistance (R_{total})		Ice resistance (R_{ice})	Height		Test No.
[m]	[N]		[N]	[m]		
	Wave water	Ice + wave	Ice – Wave	Wave	Ice	
0.03	0.76	0.99	0.23	0.021	0.023	Test15 – Test07
0.04	0.81	1.06	0.25	0.030	0.032	Test16 – Test08

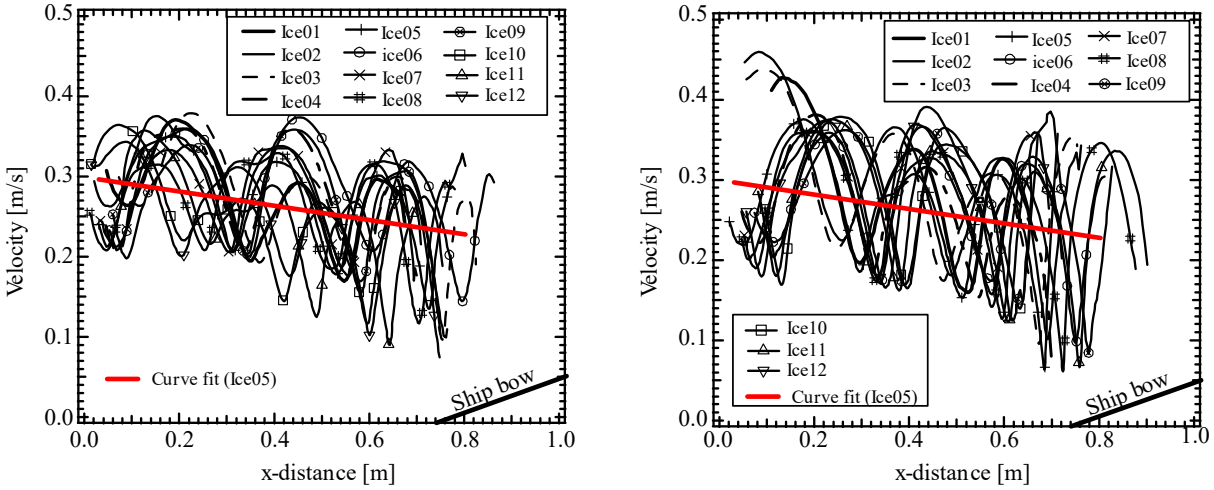

(a) Test 15 (Wave height = 0.03 m) (b) Test 16 (Wave height = 0.04 m)

Figure 7. Ice relative velocity (*x*-direction) near the ship bow in the regular wave + ice floes in different wave height.

Measured ice force and ice motion in different wave conditions.

Fig. 6 shows the resistance (average) and the peak (maximum) force in the open water (Tests 05, 07, and 08) and the ice channel (Tests 13, 15, and 16) under different wave heights. Tables 4 show the measured resistance, ice resistance obtained using Eq. (1), wave height and ice wave height. As shown in Fig. 6a, the average force in both open water and the ice channel increases proportionally with increasing wave height. On the other hand, the ice resistance remains nearly constant across different wave heights. Fig. 7 shows the ice relative velocity in the *x*-direction near the ship bow in the ice channel under wave heights of 0.03 m (Fig. 7a) and 0.04 m (Fig. 7b). In Fig.7, the ice velocities of 12 ice floes (Ice01- 12) are shown, and the trend line of the ice05 is additionally shown. A comparison between Test 15 (wave height = 0.03 m) and Test 16 (wave height = 0.04 m) reveals that the trend lines of the relative velocity are quite similar. This result indicates that the ice resistance under different wave heights is approximately the same, as shown in Fig. 6a. Based on these results, it appears that the ice resistance ($R_{\text{ice+wave}}$) in the ice channel (Tests 12, 13, 14, 15, and 16) can be estimated as the sum of the wave resistance ($R_{\text{wave (no ice)}}$) without ice (Tests 04, 05, 06, 07, and 08) and the ice resistance ($R_{\text{ice (no wave)}}$)in calm water (Tests 09, 10, and 11).

$$R_{\text{ice+wave}} = R_{\text{wave (no ice)}} + R_{\text{ice(no wave)}} \quad (2)$$

In Fig. 7, the ice relative velocity exhibits strong oscillations due to the higher wave height. The amplitude of the ice velocity oscillations increases with wave height. As shown in Fig. 6b, higher wave conditions lead to larger peak forces, induced by the increased ice velocity. These results indicate that the peak ice force under wave conditions is significantly influenced by the wave characteristics, due to their strong effect on ice motion (i.e., ice collision speed).Therefore, further experiments under various wave and ice conditions are necessary to accurately estimate the ice force (ice collision speed) in ship–ice–wave interactions

CONCLUSIONS

This study conducted model tests using synthetic ice to estimate the ice force acting on a ship advancing through small ice floes under regular wave conditions. The ice resistance in regular waves was found to be approximately equal to that in calm water, as the average ice collision velocity in regular waves appears to be similar to that in calm conditions. This suggests that the ice resistance under wave and ice conditions can potentially be estimated as the sum of the wave resistance without ice and the ice resistance in calm water. On the other hand, the peak ice force in regular waves is significantly greater than that in calm water due to the higher peak collision velocities of ice near the bow under wave conditions. The collision velocities of ice floes vary depending on the ice, wave, and ship conditions. Therefore, further experiments under a range of ice, wave, and ship conditions are required to accurately estimate the ice force under wave conditions. The effects of wave nonlinearity, ship motions under wave–ice interactions, and the differences between synthetic and natural sea ice are also considered important factors in estimating ice force, and should be addressed in future work.

ACKNOWLEDGEMENTS

This work was supported by the Arctic Challenge for Sustainability II (ArCS II), Program Grant Number JPMXD1420318865 and JSPS KAKENHI Grant Number 21KK0079 and 24K01092.

REFERENCES

Huang, L.F., Tuhkuri, J., Igrec, B., et al, 2020. Ship resistance when operating in floating ice floes: A combined CFD & DEM approach, *Mar. Struct*. 74, 102817.

Huang, L.F., Li, Z.Y., Ryan, C., et al., 2021. Ship resistance when operating in floating ice floes: derivation, validation, and application of an empirical equation, *Mar. Struct.*79, 103057.

Khon, V. C., Mokhov, I. I., Pogarskiy, F. A., Babanin, A., Dethloff, K., Rinke, A., & Matthes, H., 2014. Wave heights in the 21st century Arctic Ocean simulated with a regional climate model, *Geophysical Research Letters*, 41 (8), 2956-2961.

Luo, W.-Z., et.al., 2018. Experimental research on resistance and motion attitude variation of ship–wave–ice interaction in marginal ice zones, *Marine Structure*, 58, pp. 399-415.

Ming Zou, Xiang-Jie Tang, Lu Zou, and Zao-Jian Zoum, 2022. Numerical simulation of ship-ice interaction in pack ice area based on CFD - DEM coupling method, *OMAE 2022*-78945.

Sawamura, J., Senga H., Imaki K., Suga K. and Kim H., 2016. Ice Resistance Test using Synthetic Ice for a Ship Advancing in Ice-covered Water, *Proceeding of 23nd IAHR International Symposium on Ice*, USB

Sawamura J., et al, 2018. Ice Resistance test of a ship using synthetic ice in small pack ice floes and wave interaction, *The proceeding of 28th International Offshore and Polar Engineering Conference*, pp.1586-1590.

Tang, X., Zou, M, Zou, Z., Li, Z., Zou, L, 2022. A parametric study on the ice resistance of a ship sailing in pack ice based on CFD-DEM method, *Ocean Eng*., 265, 112563.